Magnetic Resonance Imaging 32 (2014) 184–189

Contents lists available at ScienceDirect

Magnetic Resonance Imaging

journal homepage: www.mrijournal.com

Technical notes

Advantages of QBI in TBSS analyses

Daniele Corbo [a,1], Giuseppina Caiazzo [a,1], Francesca Trojsi [a,b], Maria Rosaria Monsurrò [b], Antonio Gallo [b], Simona Bonavita [b], Gioacchino Tedeschi [a,b], Fabrizio Esposito [a,c,d,*]

[a] MRI Research Center SUN-FISM, Second University of Naples, Naples 80138, Italy
[b] Department of Medical, Surgical, Neurological, Metabolic and Aging Sciences, Second University of Naples, Naples 80138, Italy
[c] Department of Medicine and Surgery, University of Salerno, Baronissi (Salerno) 84081, Italy
[d] Department of Cognitive Neuroscience, Maastricht University, 6200 MD Maastricht, The Netherlands

ARTICLE INFO

Article history:
Received 31 July 2013
Accepted 30 September 2013

Keywords:
DTI
QBI
ALS
TBSS
Generalized Fractional Anisotropy
Fractional Anisotropy

ABSTRACT

Diffusion-weighted magnetic resonance imaging (DWMRI) is used to study white matter (WM) in normal and clinical populations. In DWMRI studies, diffusion tensor imaging (DTI) models the WM anisotropy with one dominant direction, detecting possible pathway abnormalities only in large and highly coherent fiber tracts. However, more general anisotropy models like Q-ball imaging (QBI) may provide more sensitive WM descriptors in single patients. The present study aimed to compare DTI and QBI models in a group-level population analysis, using Amyotrophic Lateral Sclerosis (ALS) as a pathological case model of WM tract degeneration.

DWMRI was performed in 19 ALS patients and 19 age and sex-matched healthy controls. DTI and QBI estimates were compared in whole-brain tract-based spatial statistics (TBSS) and volume of interest (VOI) analyses, and correlated with ALS clinical scores of disability.

A significant decrease of the QBI-derived generalized fractional anisotropy (GFA) was observed in both motor and extramotor fibers of ALS patients compared to controls. Homologue DTI-derived FA maps were only partially overlapping with GFA maps. Particularly, the left corticospinal tracts resulted more markedly depicted by the QBI than by the DTI model, with GFA predicting ALS disability better than FA.

The present findings demonstrate that QBI model is suitable for studying WM tract degeneration in population-level clinical studies. Particularly, group-level studies of fiber integrity may benefit from QBI when DTI is biased towards low values, such as in cases of fiber degeneration, and in regions with more than one dominant fiber direction.

1. Introduction

Imaging of water diffusion using magnetic resonance (MR) has become an important noninvasive method for probing white matter (WM) anatomical connectivity and integrity in the human brain for normative and clinical neuroimaging studies. Diffusion weighted MRI (DW-MRI) measurements are made sensitive to the translational diffusion of water molecules by using magnetic field gradients [1], and information about WM anisotropy can be obtained because WM fiber bundles present a barrier to diffusion that causes relatively higher diffusivity along the fiber direction, and relatively lower diffusivity across the fibers. The acquired signals depend on the strength and the direction of these diffusion-sensitizing gradients. Diffusion tensor imaging (DTI), originally formulated by Basser and colleagues [2,3], represents the most commonly used model of investigation of WM brain structure and measures the preferred direction of water diffusion along WM fiber tracts (anisotropy) [4]. Moreover, DTI allows to reconstruct cerebral connectivity "in-vivo" with the help of fiber tractography algorithms. In DTI, the neuronal fiber orientation is assumed to be collinear with the principal direction of the diffusion tensor. However, due to both resolution and signal to noise (SNR) limitations, this relationship can be anatomically ambiguous [5].

Several studies have taken advantage of the ability to study WM tract degeneration using a voxel-wise analysis of DTI-derived fractional anisotropy (FA) measures [1,6]. Quantitative FA measures are believed to reflect changes in myelination, fiber density and packing [7,8]. However, despite the development of higher performance gradient systems and multi-element phased array coils and parallel imaging in latest generation 3 T scanners, DTI of the human brain has remained seriously limited by SNR constraints. In fact the progression of new applications for diffusion imaging, while determining increasing capabilities in terms of spatial and angular

* Corresponding author. Department of Medicine and Surgery University of Salerno Via Allende, 84081 Baronissi (Salerno), Italy. Fax: +39 089 969642, +39 089 968794.
E-mail address: faesposito@unisa.it (F. Esposito).
[1] These authors contributed equally to this work.

0730-725X/$ – see front matter © 2014 Elsevier Inc. All rights reserved.
http://dx.doi.org/10.1016/j.mri.2013.09.002

resolution, has not helped to overcome some fundamental DTI shortcomings, such as the fact that DTI assumes a single major orientation within each voxel, and therefore cannot adequately handle those cases where the tissue of interest has a heterogeneous structure. This is essentially because any structure other than a single coherently oriented fiber population through that voxel cannot be modeled by DTI [9,10]. More recently, advances in image acquisition, called high angular resolution diffusion imaging (HARDI), and advances in postprocessing techniques, called Q-ball imaging (QBI), have been proposed, which allow to calculate independently several diffusion coefficients along several directions, thereby accounting for (and potentially revealing in tractography) crossing WM fibers invisible in DTI analyses [11]. This is achieved by using images obtained by diffusion-sensitizing gradients in multiple orientations (typically > 30 axes) and by using a high diffusion gradient (typically > 3000 s/mm^2). These techniques tend to require an extended data acquisition time, which may hamper their use in the clinical setting. On the other hand, as it remains possible to use QBI processing of standard DWI data, it would be interesting to see whether a more general anisotropy model produces similar or different results compared to the standard DTI anisotropy model in a given clinical population with known anisotropy abnormalities.

Among the several HARDI models, the most viable one is the QBI, which is based on the Funk–Radon transform [12] and assumes that diffusion sensitizing gradients sample the surface of a sphere at each voxel [13,14]. In QBI, the spherical function that characterizes the relative likelihood of water diffusion along any given angular direction is termed fiber orientation distribution function (ODF) [15,16]. From this function, it is possible to determine the ODF surfaces, which represent the probability of diffusion in a given direction at each voxel, and can be summarized by a generalized fractional anisotropy (GFA) coefficient for visualizing the amount of anisotropy [11,17]. Crucially, this index uses the full set of available diffusion gradients and does not rely on fitting a diffusion tensor model to the data. GFA is the most widely used QBI measure [18], and is to be considered as the QBI analog of DTI-derived FA. As QBI and DTI can be tested on the same data, in this work we aimed to investigate the advantages and the shortcomings of DTI and QBI in the analysis of a widespread WM neurodegeneration, a process that is known to be active in both motor and extra-motor pathways of amyotrophic lateral sclerosis (ALS) patients [9,19,20]. Particularly, DTI has previously enabled the assessment of the integrity of WM pathways by measuring the preferred direction of water diffusion along WM fiber tracts in terms of the FA parameter [9]. Here we compare for the first time FA and GFA estimates from ALS patients and normal healthy controls, in voxel and volume-of-interest (VOI)-based group analysis.

2. Materials and methods

2.1. Study population

We examined 19 ALS patients (9 men, 10 women; mean age 61.6 ± 11.1 years, ranging from 36 to 79 years), with definite (n = 9) or probable (n = 10) sporadic ALS, according to the Revised El Escorial criteria of the World Federation of Neurology [21]. The mean disease duration, estimated from the time of symptoms onset to the scanning, was 3.4 ± 2.6 years, ranging from 1 to 10 years. In all patients, we assessed the UMN score, a measure of pyramidal dysfunction [22]. ALS functional rating scale—revised (ALS FRS-R), an index of clinical disability [23] ranged from 45 to 18 (mean value 33.7 + 8.6). Three of the 19 patients had disease durations of >5 years and were receiving artificial respiratory support (home mechanical noninvasive ventilation; mean duration, 68 months). The control group comprised 19 healthy controls (9 men, 10 women) aged from 46 to 78 years (mean age 62.1 ± 8.5 years) with no history of neurological or psychiatric diseases and without any abnormalities detected on conventional MRI T1 and T2 weighted images. All 38 subjects included in the study were right-handed. Ethics approval for all procedures was obtained before the study. Informed consent was obtained from all participants.

2.2. MRI scanning protocol

Magnetic resonance images were acquired on a 3 T GE Medical System scanner (Signa HDxt3T twinspeed GE) equipped with an 8-channel parallel head coil. Whole-brain DTI was performed using a GRE EPI sequence (repetition time = 10000 ms, echo time = 88 ms, field of view = 320 mm, isotropic resolution = 2.5 mm, b value = 1,000 s/mm^2, 32 isotropically distributed gradients, frequency encoding RL).

2.3. DTI and Q-Ball analysis

DTI and Q-Ball imaging analysis was performed using the FMRIB FSL software package (www.fmrib.ox.ac.uk/fsl). Preprocessing included eddy current and motion correction and brain-tissue extraction. After preprocessing, DTI images were averaged and concatenated into 33 (1 B = 0 + 32 B = 1000) volumes and a diffusion tensor model was fitted at each voxel, generating FA maps, as expressed by the following equation:

$$FA = \sqrt{\frac{1}{2}\frac{\sqrt{(\lambda_1-\lambda_2)^2+(\lambda_2-\lambda_3)^2-(\lambda_3-\lambda_1)^2}}{\sqrt{(\lambda_1{}^2+\lambda_2{}^2+\lambda_3{}^2)}}} \quad (1)$$

where (λ_1, λ_2, λ_3) are the eigenvalues of the tensor.

Q-ball images were also averaged and concatenated into 33 volumes and a q-ball model was fitted at each voxel, generating GFA maps:

$$GFA = \frac{\sqrt{\left[n\sum_{i=1}^{n}(\psi_i-\langle\psi\rangle)^2\right]}}{(n-1)\sum_{i=1}^{n}(\psi_i)^2} \quad (2)$$

where ψ is the diffusion ODF vector and $\langle\psi\rangle = (1/n)\sum_{i=1}^{n}(\psi_i)$ is the mean of ODF vector [11]. DTI and Q-ball group analyses included voxel-based TBSS and atlas-based VOI analyses. For these group analyses DTI and QBI images were warped to the MNI152 template, available as standard T1 data set in the FSL software package. TBSS was run with FA and GFA maps to create the so called “skeleton”, which represents the center of all fiber bundles in common to all subjects, and which was used for all other maps [24]. To this purpose, FA and GFA images of all subjects (n = 38) were aligned to a common target (FMRIB58_FA standard space) using nonlinear registration, thereby FA and GFA maps were calculated using the FSL FMRIB's Diffusion Toolbox (FDT) tool and aligned to a 1 × 1 × 1 mm MNI152 standard space 16. To compare DTI and QBI models, a mean FA and GFA skeleton was then created with the same threshold of FA and GFA >0.1. The TBSS method projects the largest diffusion metric across the tract onto the WM skeleton, which does not account for the range of diffusivity measures within the entire WM tract. Voxel-wise correlations were performed to compare between FA and GFA on one side and UMNS on the other side. The results were shown on the skeleton map after correction for multiple comparisons with the threshold-free cluster enhancement (TFCE) technique [24]. A VOI analysis was also performed to correlate the TBSS results with standard anatomic VOI data. VOIs were defined by anatomic marks obtained from the International Consortium of Brain Mapping DTI-81 WM labels atlas (Johns Hopkins University,

Table 1
Mean value and SD of fractional anisotropy (FA) and generalized fractional anisotropy (GFA) and Pearson correlation (r) and p value between mean FA, mean GFA and upper motor neuron (UMN) score, in major fiber bundles.

Fiber bundles	FA		GFA		UMN			
	mean	SD	mean	SD	FA		GFA	
					r	p	r	p
Corpus callosum	0.306	0.057	0.187	0.008	−0.440	0.060	−0.250	0.300
Corticospinal tract	0.299	0.440	0.185	0.008	−0.453	0.051	−0.496	0.031
Superior longitudinal fasciculum	0.009	0.254	0.145	0.001	−0.220	0.360	−0.090	0.700
Fronto occipital fasciculum	0.278	0.027	0.155	0.003	0.300	0.210	0.500	0.030

Baltimore, MD) [25,26]. Individual diffusivity parameters were extracted by first aligning the specific VOI to the DTI and QBI maps of all subjects with the Nonlinear Image Registration Tool in FMRIB. Then, all subject maps were masked with this VOI, and the mean values of all diffusivity parameters were obtained. Pearson correlation coefficients were calculated to evaluate the relationship between UMN score and the mean values of all diffusivity parameters within the VOIs, and P values < 0.05 were considered statistically significant, after correction for multiple comparisons with the Bonferroni method. Quantitative measures were performed, both on the skeleton and on TBSS results maps, to compare the two models. Both skeleton maps were also segmented according to the major white matter fiber bundles, as defined in the standard WM atlas. We chose the case of complex fiber architecture, which has previously been identified by model-free inversion approaches [14,26–31]. In this way, we quantified for each fiber bundle the number of voxels for each model separately and refer these to the specific anatomical region (see Table 2). Then we quantified, in TBSS, the volume in mm^3, of the areas of differential anisotropy showed by DTI and QBI analyses, and estimated a percent difference between the two models.

3. Results

When comparing the FA skeletons of ALS patients and controls in the TBSS voxelwise analysis, a significant reduction of FA was found within the fibers of the left corticospinal tracts underneath the motor cortex and at the left ponto-mesencephalic junction, in the body of corpus callosum ($p < 0.05$, corrected for multiple comparisons) and left superior longitudinal fasciculus (Fig. 1). The QBI group analysis revealed a reduction of GFA in motor areas highly overlapping with those showed with DTI, but also a more extended involvement of the reduced anisotropy in extra-motor fiber bundles (cingulate gyrus, anterior thalamic radiations, fronto occipital fasciculus and uncinate fasciculus) ($p < 0.05$, corrected for multiple comparisons) (Fig. 1).

Table 2
Number of skeleton map voxels in DTI and Q-ball model in main fiber bundles and relative ratio.

Fiber bundles	N voxels GFA skeleton	N voxel FA skeleton	FA/GFA
Left anterior thalamic radiation	1955	1693	0.86
Right anterior thalamic radiation	40	5	0.12
Left Cingulate gyrus	16	6	0.37
Right Cingulate gyrus	1675	1230	0.73
Right Fronto-occipital fasciculus	794	728	0.92
Left Uncinate fasciculus	698	211	0.30
Right Uncinate fasciculus	260	261	1.00
Left Corticospinal-tract	2300	2402	1.04
Right Corticospinal-tract	2097	2474	1.18
Left Superior longitudinal fasciculus	1680	1431	0.85
Right Superior longitudinal fasciculus	1637	1207	0.73
Body of Corpus callosum	3404	2886	0.84

We quantified the FA and GFA skeleton structures by counting the number of voxels in major WM fiber bundles, as resulting from the TBSS analyses. Then, we estimated the volume in mm^3 of the areas of differential anisotropy showed by DTI and QBI analyses, and a percent difference between the two models, and found that GFA skeleton maps produced a different distribution of fibers compared to DTI model (Fig. 2). In the right anterior thalamic radiation, the left uncinate fasciculus and the left cingulate gyrus, QBI-derived skeleton maps revealed many more WM voxels than DTI, likely because in these ROIs there are more intersections of fibers [32,33], and therefore QBI is potentially more sensitive to the underlying ALS neurodegeneration.

Both skeleton maps were also segmented according to the major WM fiber bundles, as defined in the standard WM atlas. In this way, we could quantify for each fiber bundle the number of voxels, as yielded by each model separately and refer these to the specific anatomical region (see Table 2). We further measured the volumes of these regions resulting from the TBSS analysis: the volume of the FA pattern in the left corticospinal-tract was 4491 mm^3 while, in the same region, the pattern of GFA had a volume of 5462 mm^3, with a percent difference of 8.66% with respect to volume of the standard atlas tracts. In the left superior longitudinal fasciculus the volume difference between GFA and FA patterns, with respect to standard atlas tracts, was 47.79%, while in the body of corpus callosum, the involvement from FA to GFA regions was of 53.35%, therefore in the regions of overlap of TBSS results QBI shows regions of differences which are more extended in volume (see Table 3).

The Pearson correlation analyses showed a significant negative correlation between both individual regional FA and GFA values and UMN scores at the left ponto mesencephalic junction within the corticospinal tracts. In this region, when comparing DTI and QBI models, GFA correlation values with UMN scores were significantly higher than FA correlation values in the patients group, in fact FA yielded a correlation of −0.453 while GFA a value of −0.496 (see Table 1).

4. Discussion

In this study we compared TBSS analyses starting from FA and GFA skeleton maps of ALS patients and healthy subjects. HARDI techniques in general, and specifically the QBI model, have been previously used in clinical studies [10,34,35]. On the other hand, the possibility that QBI-derived GFA maps can be used in group studies like DTI-based FA-maps is grounded on these studies: for instance, with regard to cortico-motor networks, multitensor tractography using a standard b-value (1000 s/mm^2) has proven more powerful than DTI in depicting the fiber tracts from the face and tongue regions of the primary motor cortex compared to DTI-based tractography in patients with brain tumors [10]. Therefore, a multi-fiber tractography, as made by possible by QBI, can be more sensitive to non-dominant projections than single fiber DTI-based tractography, especially in the medial portion of the superior longitudinal fasciculus and in other cases where false negatives in single-fiber

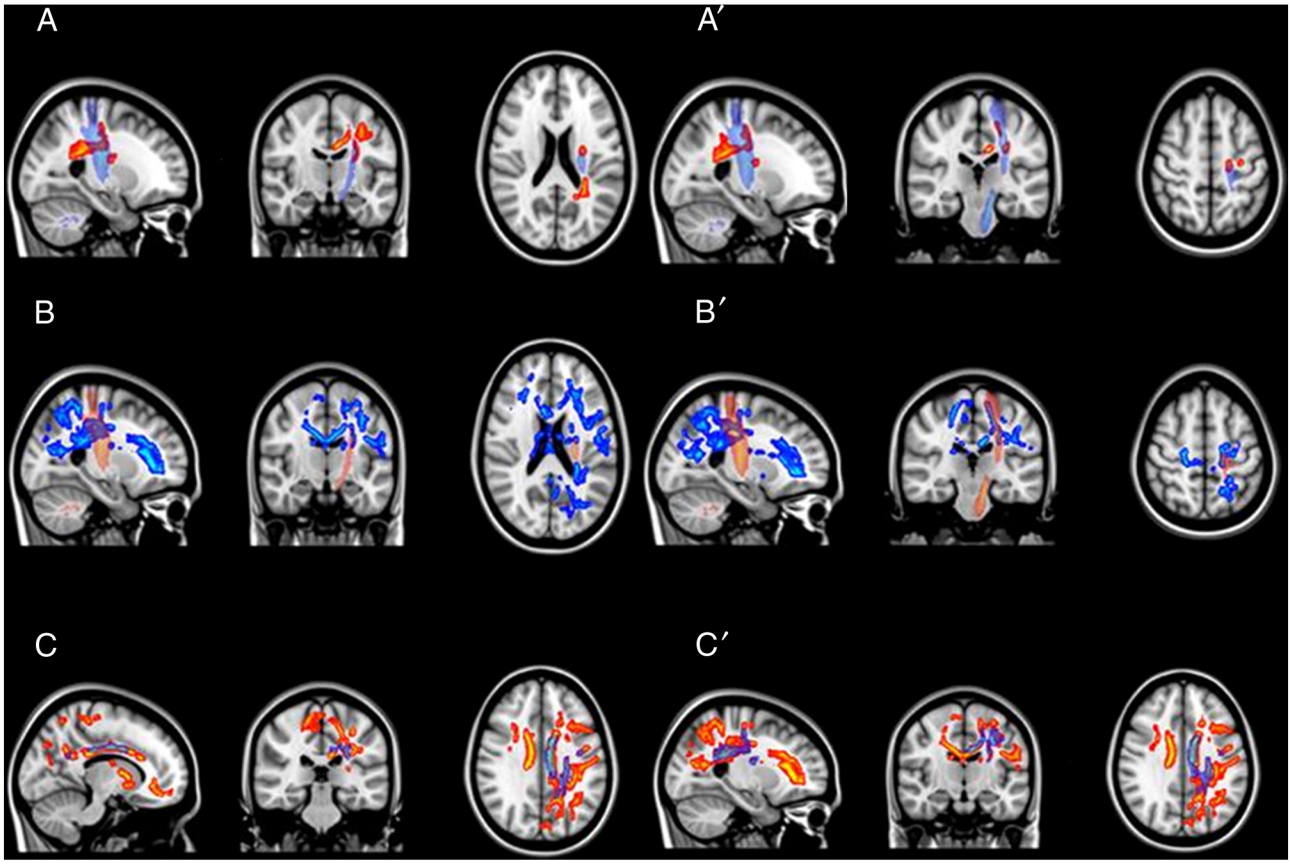

Fig. 1. A/A'. TBSS analysis of FA maps generated for the ALS and control participants. The red–yellow regions show where there was a significant reduction in FA value in ALS patients, corrected for multiple comparisons ($p < 0.05$). In the two last pictures the blue region show the corticospinal tract ROI from the FSL JHU with matter labels. B/B'. TBSS analysis of GFA maps generated for the ALS and control participants. The blue regions show where there was a significant reduction in GFA value in ALS patients, corrected for multiple comparisons ($p < 0.05$). In the two last pictures the red region show the corticospinal tract ROI from the FSL JHU with matter labels. C/C'. TBSS analysis of GFA data in red and FA data in blue corrected for multiple comparisons ($p < 0.05$).

tractography are due to difficulties in tracing a nondominant pathway [28].

Our findings obtained by using voxel-wise analyses of FA maps corroborate previous evidence [35–37], showing pathway of WM degeneration in multiple motor networks in patients with ALS. We thus used the QBI model to generate GFA maps instead of FA maps and submitted these maps exactly to the same TBSS pipeline. This new analysis showed a more extended pathway of ALS degeneration, involving extra-motor fiber bundles that appeared normal in the DTI analysis.

The depiction of the motor pathway by using a conventional DTI model was in fact limited to only part of the entire corticospinal tracts because the major fiber bundles, such as the callosal fibers and superior longitudinal fascicles, were likely crossing the motor tract at

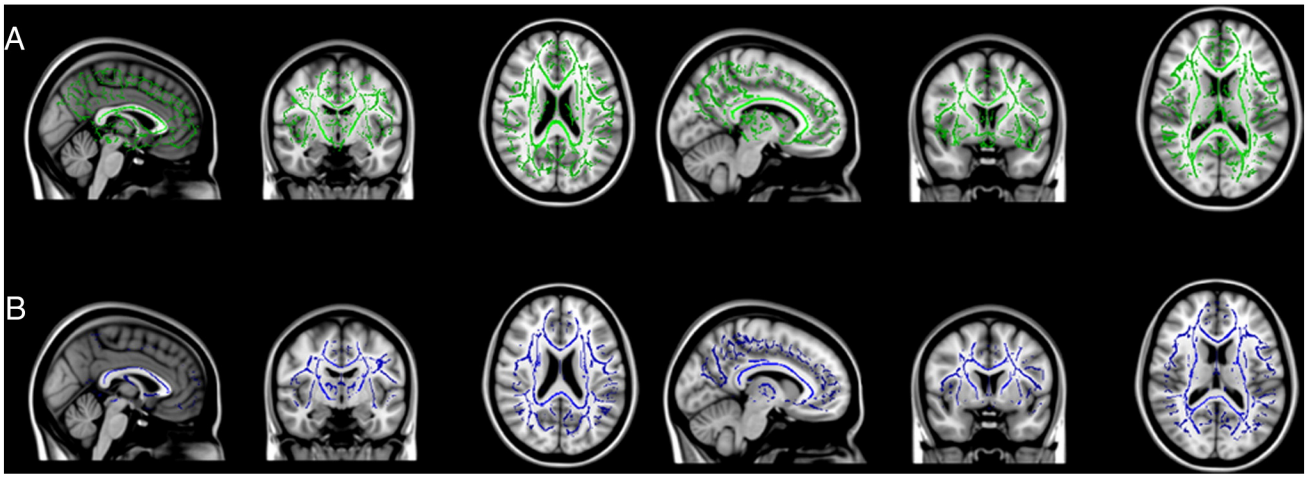

Fig. 2. A. GFA skeleton map (green). B. FA skeleton map (blue).

Table 3
TBSS results in major fiber bundles: bundles volumes with significant difference between ALS patients and controls in both DTI and Q-ball models.

Fiber bundles	Volume (mm^3) DTI	Volume(mm^3) HARDI
Left Corticospinal-tract	4491	5462
Left Supirior Longitudinal fasciculus	415	3573
Body of Corpus callosum	2133	9449

the level of the centrum semiovale. When these fiber bundles intersect within a voxel, the DTI model was probably not sufficient to comprehensively describe the anatomical connectivity of this voxel. On the other hand, a DTI underestimation of motor fibers because of crossing fibers has been clearly observed in patients with axonal lesions [11]. For what concerns the corpus callosum (CC) investigation, previous tractographic results obtained with both DTI and QBI in cases of partial agenesia of the CC [38] have demonstrated a remarkable diversity of callosal connectivity, including a number of heterotopic tracts that were absent in healthy subjects. As a consequence, more tracts and more extensive fibers within these tracts can be potentially recovered with QBI than with DTI and this expectation was confirmed by our results.

DTI and HARDI postprocessing approaches have been also compared in congenital brain malformations, such as horizontal gaze palsy with progressive scoliosis, pontine tegmental cap dysplasia, holoprosencephaly [39]. Even at the spinal level, where DW-MRI is challenging due to the small cross-sectional size of the cord and the presence of physiological motion and susceptibility artifacts, HARDI results overcame these limitations and allowed to study Wallerian degeneration in case of spinal trauma [16].

One potential caveat in comparing DTI and QBI models in group studies is that the derived anisotropy parameters are based on different mathematical models which, if applied to the same data set, normally generate different values in each voxel. Particularly, GFA values are expected to be lower than FA values because the former need to account for many more directions than the latter. Nonetheless, it has been shown that GFA and FA have a linear dependence in brain in-vivo measurements [15,33], allowing for statistical pooling of these parameters from the individual to the population level. In our study, to compare the two models of the same distribution of fibers' orientation, we have determined the skeleton maps from both FA or GFA maps, calculated the differences between patients and controls in these skeletons, and quantified the overlap of the regional differences with the standard distribution of the main WM tracts, as obtained from the atlas. As expected, we found that the main differences between the two models in TBSS results where in regions supposed or known to have many fiber crossings, such as right anterior thalamic radiation, left cingulate gyrus and left uncinate fasciculus [28]. Therefore, QBI derived distributions can make TBSS more sensitive to detect group differences.

With regard to ALS, as a model of neurodegeneration, it is nowadays fully acknowledged that ALS pathology is widespread and involves both motor and extramotor networks [40]. In previous studies, a voxelwise approach based on whole-brain TBSS DTI analysis has resulted in improved accuracy in detecting distributed microstructural disease-related WM changes [6,27]. Here, we explored the whole-brain GFA changes in ALS using a QBI approach, providing further evidence about the actual extent of the neurodegenerative process. A previous study exploring WM pathways in ALS by using HARDI and whole brain probabilistic tractography has also reported abnormal connectivity pathways in both motor and extra-motor networks in single patients [34]. Along this direction, we also correlated individual GFA and FA values with a clinical index (UMN score) and found that GFAs correlate better than FAs with UMNs in left corticospinal tract, whereas this was not the case in CC. Therefore, in regions with a homogeneous and coherent fiber configuration, where the individual tracts are large enough to avoid partial volume effects with other structures at the used voxel resolution, such as in the body of the CC DTI-based FA quantification can be more sensitive than QBI-based GFA. More in general, the choice between DTI-based FA and QBI-based GFA quantification can be dependent on the aim of the research and the target WM region. Particularly, clinical studies of fiber integrity may benefit from HARDI, when DTI-derived measures of anisotropy are biased towards low values, which happen in about 40% of WM voxels, and where more than one dominant fiber direction can be detectable [32,33]. In fact, FA becomes less advantageous where there are complex crossing fibers, such as in the left superior longitudinal tract.

Finally, it should be remarked that QBI has been not exploited here to its maximal potentials for WM tractography, which would require the use of high b-value DWMRI measurements [41]. Using high b-values would be useful (and necessary) to differentiate the different diffusion compartments according to the intra-voxel orientational heterogeneity conditions [16]. In this study, however, we wanted to compare the performances of QBI and DTI not for tractographic purposes, but for voxel-wise group-level analyses within the TBSS framework, and therefore a standard b-value was used, so that the acquisition time was relatively low. In this way the advantages showed from the analysis were due only to the models, not to the HARDI sequence. Recent work has shown that it is important to model diffusivity relative to fiber orientation; making full use of the HARDI based acquisition [42], therefore in the future we will assess the performances of DTI and QBI in group studies using HARDI sequences.

Acknowledgments

The authors thank Antonella Paccone for technical assistance.

References

[1] Abe O, Yamada H, Masutani Y, Aoki S, Kunimatsu A, Yamasue H, et al. Amyotrophic lateral sclerosis: diffusion tensor tractography and voxel-based analysis. NMR Biomed 2004;17(6):411–6.
[2] Basser PJ, Mattiello J, LeBihan D. Estimate of the effective self-diffusion tensor from the NMR spin echo. J Magn Reson 1994;Vol.B(no. 103):247–54.
[3] Basser PJ, Pajevic S, Pierpaoli C, Duda J, Aldroubi A. In vivo fiber tractography using DT-MRI data. Magn Reson Med 2000;44:625–32.
[4] Beaulieu C. The basis of anisotropic water diffusion in the nervous system — a technical review. NMR Biomed 2002;15:435–55.
[5] Ozarslan Evren, Shepherd Timothy M, Vemuri Baba C, Blackband Stephen J, Mareci Thomas H. Fast orientation mapping from HARDI. Med Image Comput Comput Assist Interv Int Conf Med Image Comput Comput Assist Interv 2005;8:156–63.
[6] Ciccarelli O, Behrens TE, Altmann DR, Orrell RW, Howard RS, Johansen-Berg H, et al. Probabilistic diffusion tractography: a potential tool to assess the rate of disease progression in amyotrophic lateral sclerosis. Brain 2006;129:1859–71.
[7] Concha L, Livy DL, Beaulieu C, Wheatley BM, Gross DW. In vivo diffusion tensor imaging and histopathology of the fimbria–fornix in temporal lobe epilepsy.J. Neurosciences 2010;30(3):996–1002.
[8] Filippini N, Douaud G, Mackay CE, Knight S, Talbot K, Turner MR. Corpus callosum involvement is a consistent feature of amyotrophic lateral sclerosis. Neurology 2010;75(18):1645–52.
[9] Alexander DC, Barker GJ, Arridge SR. Detection and modeling of non-Gaussian apparent diffusion coefficient profiles in human brain data. Magn Reson Med 2002;48(2):331–40.
[10] Yamada K, Sakai K, Hoogenraad FG, Holthuizen R, Akazawa K, Ito H, et al. Multitensor tractography enables better depiction of motor pathways: initial clinical experience using diffusion-weighted MR imaging with standard b-value. AJNR Am J Neuroradiol 2007(9):1668–73.
[11] Tuch DS. Q-ball imaging. Magn Reson Med 2004;52:1358–72.
[12] Hess CP, Mukherjee P, Han ET, Xu D, Vigneron DB. Q-ball reconstruction of multimodal fiber orientations using the spherical harmonic basis. Magn Reson Med 2006;56(1):104–17.
[13] Tuch DS, Weisskoff RM, Belliveau JW, Wedeen VJ. High angular resolution diffusion imaging of the human brain. In Proc. Of the 7th Annual Meeting of ISMRM, Philadelphia, PA; 1999. p. 321.

[14] Tuch DS, Reese TG, Wiegell MR, Wedeen VJ. Diffusion MRI of complex neural architecture. Neuron 2003;40:885–95.
[15] Gorczewski K, Mang S, Klose U. Reproducibility and consistency of evaluation techniques for HARDI data. MAGMA 2009;22:63–70.
[16] Cohen-Adad J, Descoteaux M, Wald LL. Quality assessment of high angular resolution diffusion imaging data using bootstrap on Q-ball reconstruction. J Magn Reson Imaging 2011;33(5):1194–208.
[17] Hagmann P, Kurant M, Gigandet X, Thiran P, Wedeen VJ, Meuli R, Thiran JP. Mapping human whole brain structural networks with diffusion MRI. PLoS ONE 2007;2(7):597.
[18] Fritzsche KH, Laun FB, Meinzer HP, Stieltjes B. Opportunities and pitfalls in the quantification of fiber integrity: what can we gain from Q-ball imaging? Neuroimage 2010;51(1):242–51.
[19] Agosta F, Pagani E, Petrolini M, Caputo D, Perini M, Prelle A, et al. Assessment of white matter tract damage in patients with amyotrophic lateral sclerosis: a diffusion tensor MRI imaging tractography study. AJNR Am J Neuroradiol 2010;31:1457–61.
[20] Mädler B, Drabycz SA, Kolind SH, Whittall KP, MacKay AL. Is diffusion anisotropy an accuratemonitor ofmyelination? Correlation ofmulticomponent T2 relaxation and diffusion tensor anisotropy in human brain. Magn Reson Imaging 2008;26:874–88.
[21] Brooks BR, Miller RG, Swash M, et al. El Escorial revisited: revised criteria for the diagnosis of amyotrophic lateral sclerosis. Amyotroph Lateral Scler Other Motor Neuron Disord 2000;1:293–9.
[22] Kaufmann P, Pullman SL, Shungu DC, et al. Objective tests for upper motor neuron involvement in amyotrophic lateral sclerosis (ALS). Neurology 2004;62:1753–7.
[23] Cedarbaum JM, Stambler N, Malta E, Fuller C, Hilt D, Thurmond B, et al. The ALSFRS-R: a revised ALS functional rating scale that incorporates assessments of respiratory function: BDNF ALS Study Group (Phase III). J Neurol Sci 1999;169:13–21.
[24] Smith SM, Jenkinson M, Johansen-Berg H, Rueckert D, Nichols TE, Mackay CE, et al. Tract-based spatial statistics: voxelwise analysis of multi-subject diffusion data. Neuroimage 2006;31:1487–505.
[25] Hua K, Zhang J, Wakana S, et al. Tract probability maps in stereotaxic spaces: analysis of white matter anatomy and tract-specific quantification. Neuroimage 2008;39:336–47.
[26] Kinoshita T, Moritani T, Hiwatashi A, Wang HZ, Shrier DA, Numaguchi Y, et al. Conspicuity of diffuse axonal injury lesions on diffusion-weighted MR imaging. Eur J Radiol 2005;56(1):5–11.
[27] Behrens TEJ, Woolrich MW, Jenkinson M, Johansen-Berg H, Nunes RG, Clare S, Matthews PM, Brady JM, Smith SM. Characterization and propagation of uncertainty in diffusion-weighted MR imaging. Magn Reson Med 2003;50:1077–88.
[28] Behrens TE, Berg HJ, Jbabdi S, Rushworth MF, Woolrich MW. Probabilistic diffusion tractography with multiple fibre orientations: What can we gain? Neuroimage 2007;34(1):144–55.
[29] Tournier JD, Calamante F, Gadian DG, Connelly A. Direct estimation of the fiber orientation density function from diffusion-weighted MRI data using spherical deconvolution. Neuroimage 2004 Nov;23(3):1176–85.
[30] Turner MR, Modo M. Advances in the application of MRI to amyotrophic lateral sclerosis. Expert Opin Med Diagn 2010;4(6):483–96.
[31] Vaessen MJ, Hofman PA, Tijssen HN, Aldenkamp AP, Jansen JF, Backes WH. The effect and reproducibility of different clinical DTI gradient sets on small world brain connectivity measures. Neuroimage 2010;51(3):1106–16.
[32] Wakana S, Caprihan A, Panzenboeck MM, et al. Reproducibility of quantitative tractography methods applied to cerebral white matter. Neuroimage 2007;36:630–44.
[33] Zhan L, Leow AD, Jahanshad N, Chiang MC, Barysheva M, Lee AD, et al. How does angular resolution affect diffusion imaging measures? Neuroimage 2009;49:1357–71.
[34] Rose S, Pannek K, Bell C, Baumann F, Hutchinson N, Coulthard A, et al. Direct evidence of intra- and interhemispheric corticomotor network degeneration in amyotrophic lateral sclerosis: an automated MRI structural connectivity study. Neuroimage 2012;59(3):2661–9.
[35] Trojsi F, Corbo D, Caiazzo G, Piccirillo G, Monsurrò MR, Cirillo S, et al. Motor and extramotor neurodegeneration in amyotrophic lateral sclerosis: A 3 T high angular resolution diffusion imaging (HARDI) study. Amyotroph Lateral Scler Frontotemporal Degener 2013.
[36] Cirillo M, Esposito F, Tedeschi G, Caiazzo G, Sagnelli A, Piccirillo G, et al. Widespread microstructural white matter involvement in amyotrophic lateral sclerosis: a whole-brain DTI study. AJNR Am J Neuroradiol 2012;33(6):1102–8.
[37] Jansons Kalvis M, Alexander Daniel C. Persistent angular structure: new insights from diffusion MRI data. Dummy version. Inf Process Med Imaging 2003;18:672–83.
[38] Wahl M, Strominger Z, Jeremy RJ, Barkovich AJ, Wakahiro M, Sherr EH, et al. Variability of homotopic and heterotopic callosal connectivity in partial agenesis of the corpus callosum: a 3 T diffusion tensor imaging and Q-ball tractography study. AJNR Am J Neuroradiol 2009;30(2):282–9.
[39] Wahl M, Barkovich AJ, Mukherjee P. Diffusion imaging and tractography of congenital brain malformations. Pediatr Radiol 2010;40(1):59–67.
[40] Eisen A, Weber M. Neurophysiological evaluation of cortical function in the early diagnosis of ALS. Amyotroph Lateral Scler Other Motor Neuron Disord 2000;1(Suppl 1):S47–51.
[41] Tournier JD, Calamante F, Connelly A. Robust determination of the fibre orientation distribution in diffusion MRI: non-negativity constrained super-resolved spherical deconvolution. Neuroimage 2007;35(4):1459–72.
[42] Raffelt D, Tournier JD, Rose S, Ridgway GR, Henderson R, Crozier S, et al. Apparent Fibre Density: a novel measure for the analysis of diffusion-weighted magnetic resonance images. Neuroimage 2012;15;59(4):3976–94.